Journal of Membrane Science 621 (2021) 119004

Contents lists available at ScienceDirect

Journal of Membrane Science

journal homepage: http://www.elsevier.com/locate/memsci

Performance enhancement of a submerged vacuum membrane distillation (S-VMD) system using low-power ultrasound

Ahmad Bamasag [a,b,1], Hooman Daghooghi-Mobarakeh [b,1], Talal Alqahtani [c], Patrick Phelan [b,*]

[a] Faculty of Engineering, Department of Mechanical Engineering, King Abdulaziz University (KAU), Jeddah, Saudi Arabia
[b] School for Engineering of Matter, Transport & Energy (SEMTE), Arizona State University (ASU), Tempe, AZ, United States
[c] College of Engineering, Mechanical Engineering Department, King Khalid University, Abha, Saudi Arabia

ARTICLE INFO

Keywords:
Submerged membrane distillation
Vacuum membrane distillation
Ultrasound
Acoustic cavitation
Acoustic frequency

ABSTRACT

Submerged vacuum membrane distillation (S-VMD) is a thermally driven separation process capable of desalinating water with high salt concentration. Agitation techniques such as aeration and circulation have been used to enhance the permeate flux and to mitigate the effect of temperature and concentration polarizations, a major drawback in S-VMD. In this study, an S-VMD system that uses ultrasonic energy as an agitation technique is proposed. The effects of ultrasonic power and frequency under different feed temperatures and concentrations were investigated experimentally. Results show that applying low-power ultrasound can improve the permeate flux up to 24% compared to the same process without ultrasonic energy under the same operating conditions. The ultrasound-assisted enhancement increases with higher ultrasonic power and lower frequency, as well as lower feed temperature and higher concentration. Possible heat and mass transfer enhancement mechanisms associated with integration of ultrasound were investigated and based on the variation of the permeate flux with frequency, the enhancement was mainly attributed to acoustic cavitation. The ultrasonic-assisted S-VMD system maintained a stable permeate flux and excellent water quality over a relatively long-term operation, indicating that ultrasonic energy is a promising and safe method to enhance the permeate flux in S-VMD systems.

1. Introduction

Membrane distillation (MD) is a thermally driven desalination method that uses a microporous hydrophobic membrane as a physical barrier between a hot feed side (e.g. seawater or inland water) and a cold permeate side [1,2]. Vapor transfers from the feed side to the permeate side as a result of the difference in partial pressure across the membrane wall. The vapor can either condense inside the MD modules as in direct contact MD (DCMD) and air gap MD (AGMD) configurations, or in an external condenser as in sweeping gas MD (SGMD) and vacuum MD (VMD) configurations [3].

MD can be classified on the basis of the feed water mechanism into cross-flow and submerged configurations. Cross-flow MD systems are considered the default configuration, where the feed is pumped through an MD module with feed inlet and outlet. Recently, researchers have suggested a submerged MD (S-MD) configuration, where the membranes are directly submerged within the feed tank that is heated by an electric heating element. This eliminates the need for circulating pumps and minimizes heat loss that exists in the cross-flow configuration due to recirculation and reheating. S-MD has been mainly applied to treat high concentration feed water such as inland brine [4,5], seawater RO brine [6], and coal-seam-gas-produced water [7].

One major drawback of S-MD systems is that they lack feed turbulence, which may worsen the effects of temperature and concentration polarizations, leading to lower permeate flux and faster membrane fouling. Therefore, various agitation techniques were applied to tackle this challenge, including transverse vibration [4,5,8], stirring [6,8,9], and aeration [4,5]. These methods reportedly enhanced permeate flux and reduced membrane fouling and scaling. For example, Meng et al. found that, in a submerged VMD system, applying transverse vibration can improve the permeate flux by 21% compared to the case without agitation [4]. More recently, Bamasag et al. found that circulation and aeration can significantly improve the permeate flux in submerged VMD [10].

One potential enhancement method that has not been studied in S-MD systems yet is ultrasound. In fact, ultrasound energy has been used to enhance thermal-based processes such as heat exchangers, phase

* Corresponding author.
E-mail address: phelan@asu.edu (P. Phelan).
[1] These authors contributed equally to this work.

https://doi.org/10.1016/j.memsci.2020.119004
Received 27 October 2020; Received in revised form 17 December 2020; Accepted 20 December 2020
Available online 23 December 2020

Nomenclature

A_m	Membrane effective surface area (m^2)
b	Transducer radius (m)
c	Speed of sound (m s^{-1})
C_p	Specific heat capacity (J kg^{-1} $^oC^{-1}$)
E_T	Acoustic energy delivered by transducer (J)
F	Kinematic momentum (kg^2 m^{-2} s^{-2})
f	Ultrasonic frequency (kHz)
I	Acoustic intensity (W m^{-2})
I_{rms}	Root mean square current (A)
J	Permeate flux (kg m^{-2} h^{-1})
K	Mass transfer coefficient (kg Pa^{-1} m^{-2} h^{-1})
$\dot{m}_d$	Distillate water mass (kg)
$\dot{m}_{HTF}$	Mass flow rate of the heat transfer fluid (kg/s)
P_a	Acoustic pressure (Pa)
P_b	Bubble pressure (Pa)
$P_{f,m}$	Feed vapor pressure at the membrane surface (Pa)
P_h	Hydraulic pressure (Pa)
P_l	Fluid instantaneous pressure (Pa)
P_{max}	Bubble maximum pressure (Pa)
P_v	Vacuum pressure (Pa)
$\dot{Q}_{heat}$	Supplied heat rate (W)
SEC	Specific energy consumption (kWh kg^{-1})
$SEEC$	Specific electric energy consumption (kWh kg^{-1})
$STEC$	Specific thermal energy consumption (kWh kg^{-1})
$T_{f,b}$	Feed temperature at the bulk phase (^oC)
$T_{f,m}$	Feed temperature at the membrane surface (^oC)
T_{max}	Bubble maximum temperature (K)
ΔT_{HTF}	Temperature drop of the heat transfer fluid (^oC)
$UESEC$	Ultrasonic enhanced specific energy consumption (−)
V_{rms}	Root mean square voltage (V)
x	Distance from transducer (cm)
$\dot{W}$	Electric power (W)
$\dot{W}_{US}$	Ultrasonic power (W)
$\dot{W}_{vaccum}$	Vacuum pump power (W)

Greek letters

Φ	Permeate flux enhancement ratio (−)
θ	Phase angle (Rad)
ρ	Density (kg m^{-3})
α	Acoustic attenuation coefficient (m^{-1})
ω	Angular frequency (Rad)
γ	Specific heat ratio (−)
σ	Surface tension (Nm^{-1})
μ	Dynamic viscosity (Pa.s)
δ	Acoustic displacement (m)

Abbreviations

AGMD	Air gap membrane distillation
DCMD	Direct contact membrane distillation
MD	Membrane distillation
SGMD	Sweeping gas membrane distillation
S-MD	Submerged membrane distillation
S-VMD	Submerged vacuum membrane distillation
VMD	Vacuum membrane distillation

change, and desorption processes [11–13]. Moreover, ultrasound was integrated before with membrane-based water treatment technologies such as Ultrafiltration (UF) and Microfiltration (MF) mainly to mitigate membrane fouling [14]. More relevantly, ultrasound irradiation has been integrated before with conventional cross-flow MD systems under the AGMD [15,16] and DCMD [17] configurations. Generally speaking, ultrasound was found to be effective in increasing the permeate flux and reducing membrane fouling and scaling.

To our knowledge, the first work that integrated ultrasound with MD was conducted by Zhu et al. [16]. They found that the permeate flux in an ultrasonic-assisted AGMD system can be improved by up to 25% compared to that with no ultrasonic irradiation. The improvement was attributed to a reduction in the temperature polarization caused by microstreaming and cavitation mechanisms.

Hou et al. studied the performance of an ultrasonic-assisted DCMD process using hollow fiber membranes [17]. It was reported that the permeate flux can be enhanced between 5% and 60% depending on the operating conditions. The enhancement ratio (i.e. the ratio of the permeate flux with ultrasound to that without ultrasound) can be enlarged at lower feed temperature and velocity, and low frequency as well as higher feed concentration and higher ultrasonic power. In subsequent studies, the same group illustrated how the use of US can mitigate $CaSO_4$ membrane scaling [18] and silica fouling [19] and maintain a more stable permeate flux in a DCMD system.

Recently, Naji et al. studied the effect of directly attached low-power ultrasound on the performance of a cross-flow AGMD using a flat sheet membrane [15]. The authors reported an enhancement on the permeate flux after extended operation, which was attributed only to the acoustic streaming effects that improved mass transfer and membrane cleaning.

It is worth noting that ultrasound was also used as an off-line membrane cleaning method. Hejazi et al. reported that ultrasonic cleaning helped to restore the hydrophobicity of used membranes [20]. Cho et al. applied ultrasonic cleaning on fouled membranes, and they found it is more efficient in removing membrane foulants and recovering the flux when compared to conventional physical and chemical cleaning techniques [21]. However, the authors reported a structural damage or wetting of the MD membranes when high ultrasonic power at low frequencies (150 and 300 W at 28 and 45 kHz) are used.

The goal of this paper is to experimentally investigate the use of ultrasonic energy as an agitation technique in a submerged vacuum membrane distillation (S-VMD) system. The effect of ultrasonic power and frequency on the permeate flux with different feed temperatures and concentrations will be studied. The enhanced transport phenomena associated with application of ultrasound in the S-VMD systems are investigated and mechanisms which dominantly contribute are identified and quantified. In addition, a relatively long-duration test was conducted to investigate the effect of ultrasound on the permeate flux and water quality. Finally, an energy consumption analysis was performed. The paper represents the first attempt to apply ultrasonic energy in an S-VMD system, and it will add substantially to our understanding of integrating ultrasound with different MD processes.

2. Materials and methodology

2.1. Membrane and module specifications

Fig. 1 shows a schematic and a photograph of the proposed US-assisted S-VMD system. A membrane module is submerged in a container filled with feed water, which is heated internally by a tubing coil. An ultrasonic transducer is directly attached to the bottom of the feed container. The module consists of eight hydrophobic capillary membranes with effective length of 9.7 ± 0.1 cm and a surface area of 43.9 ± 0.5 cm^2. The membranes were potted manually using epoxy resin with a "dead-end" bottom side and a top side connected to the vacuum line. The physical characteristics of the membranes and the container are shown in Table 1.

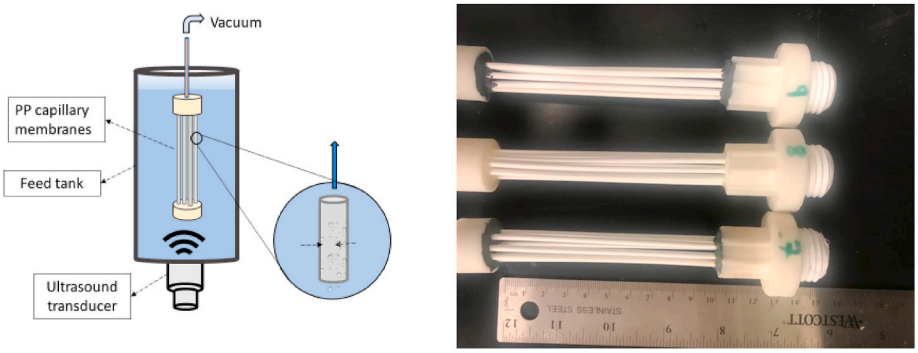

Fig. 1. A schematic diagram (left) and a photograph (right) of the S-VMD modules.

Table 1
Characteristics of the S-VMD module.

Membrane manufacturer	Microdyn-Nadir
Membrane material	Polypropylene
Pore size (μm)	0.2
Porosity	0.7
Tortuosity	1.4
Capillary inner diameter (mm)	1.8
Capillary outer diameter (mm)	2.7
Capillary thickness (μm)	450
Number of membrane capillaries	8
Length of membrane (cm)	9.7
Membrane surface area A_m (m^2)	0.0044
Container diameter (cm)	7.3
Container length (cm)	15
Container capacity (L)	0.55

2.2. Experimental setup and procedure

A schematic diagram of the experimental setup is shown in Fig. 2. The feed solution is heated by a tubing coil with pure water as the heat transfer fluid. The pure water is circulated by a temperature-controlled hot water bath (Thermo Haake DC 10-P5), which is adjusted to achieve the required feed temperature. In contrast to the conventional heating method in S-VMD which uses an electric immersion heating element placed on the top of the container, the heating method in the current design provides a more uniform thermal distribution and ensures consistent heat supply in all experimental runs.

Considering the diameter of the heating coil relative to the diameter of the feed tank and the feed tank's height relative to its radius ($O(L_{FT}/r_{FT})\tilde{}10$), radial temperature measurement was deemed to be unnecessary. The feed solution temperature was measured at two different locations using OMEGA K- type thermocouples (wire diameter = 0.571 mm), referred to as top-axial and bottom-axial temperatures, and a NATIONAL INSTRUMENTS data acquisition device NI cDAQ-9171.

A vacuum pump is used to create a vacuum pressure (-93.5 ± 0.5 kPa) on the permeate side of the membranes. The pressure was monitored using a digital pressure gauge. An external condenser liquefies the water vapor generated by the distillation process using cold pure water at 5 °C, which is supplied by a thermal circulating bath (Col-Parmer EW-12122-42). The amount of distillate water is measured using an electronic scale. The permeate flux J (in $kg{\cdot}m^{-2}{\cdot}h^{-1}$) is calculated as:

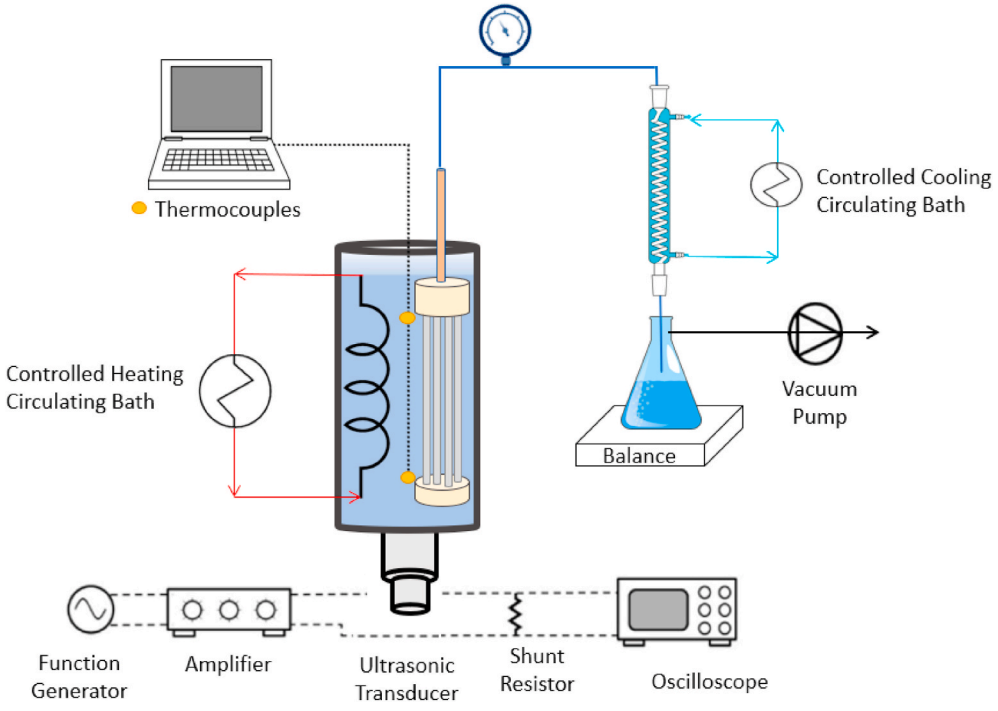

Fig. 2. A schematic diagram of the experimental setup.

$$J = \frac{m_d}{A_m \Delta t} \quad (1)$$

where m_d is the amount of distillate water (kg), A_m the membrane area (m^2), and t the sampling period (h). The permeate water quality is measured by a portable electrical conductivity meter (HM EC-3).

The main constituent elements of the ultrasonic unit used in this study are a function generator (Siglent Technologies SDG1032X), a high frequency-low slew rate amplifier (AALABSYSTEMS A-303), a shunt resistor and two ultrasonic power transducers of different resonant frequencies. The ultrasonic power transducers used are of low-heat, high-efficiency piezoceramic type acquired from APC INTERNATIONAL, LTD. The ultrasonic transducer and the shunt resistor were connected in series and with the help of four voltage probes, the impedance of the transducer based on the voltages across the transducer and across the shunt resistor was measured. The resonant frequency corresponds to the lowest impedance (also the phase difference between the voltage and current is zero). The resonant frequencies of the unloaded transducers given by the supplier, 28 kHz-50 W (APC 90–4040) and 40 kHz-50 W (APC 90–4050), were verified and the resonant frequencies of the loaded transducer-feed tank assembly were determined to be 27.55 and 39.65 kHz, respectively. Instead of using a commercially available ultrasonic generator with a fixed or limited power and frequency output, an integration of function generator and amplifier which allows for the transducer to be powered at any desirable power level and frequency was used. The ultrasonic power was determined as:

$$P_{US} = V_{rms}\, I_{rms} \cos\theta \quad (2)$$

where V_{rms} is the root mean square voltage across the transducer, I_{rms} the root mean square alternating current passing through the transducer, and θ the phase angle between the voltage and current. In order to avoid any structural damage and in consideration of minimizing energy consumption, low levels of ultrasonic power of only 10 and 30 W were considered [15].

Short-term experimental runs with and without applying ultrasound were conducted to study the enhancement effect of ultrasonic power and frequency on the permeate flux. Each short-term experimental run lasted for 25 min. The ultrasonic transducer operated continuously in these tests. Different feed temperatures (45, 55, and 65 °C) and different feed concentration (pure water, 35, 100, 200 g/l) were tested. At the completion of each experimental run, the membranes are taken outside the container to be rinsed and cleaned.

A similar experimental procedure was conducted to measure the effect of ultrasound on permeate flux and quality for a relatively long operation. At the end of these tests, the membranes were characterized with scanning electron microscopy (SEM) using Philips (Model XL 30) and Energy Dispersive X-Ray Spectroscopy (EDS) using EDAX Detector (Model 132–10).

2.3. Uncertainty analysis

The accuracy of the measured variables was calculated to be ±0.01 g, ± 0.4 °C, and ±0.5 cm^2 for mass, temperature, and membrane surface area, respectively. The vacuum pressure and feed temperature were controlled within ±0.5 kPa and 0.5 °C, respectively. To show a reasonable reproducibility, repeated readings were obtained with a maximum standard deviation of 2.7%. To determine the errors in the calculated variables (i.e. J and Φ), the expanded uncertainty method was adopted to achieve a high level of confidence (~95%) [22]. The details of the uncertainty analysis are presented in a previous work [23].

3. Results and discussion

3.1. The performance of the ultrasonic-assisted S-VMD with feed temperature

The effect of the ultrasonic power and frequency on the permeate flux (J) under steady-state operating conditions was measured. The bulk feed temperature $T_{f,b}$ was kept at 45, 55, and 65 °C, and a 35 g/l NaCl solution was used as the feed water (TDS of standard seawater). The experiments were carried out with and without ultrasonic energy at two levels of power (10 and 30 Watts) and two values of frequency (28 and 40 kHz).

The values of J as a function of the feed temperature (±0.5 °C) with and without ultrasonic energy at a frequency of 40 kHz and 28 kHz are shown in Fig. 3(a) and (b), respectively. As expected, in all cases, higher values of J are achieved with higher feed temperature. This is because J increases linearly with the difference in the vapor partial pressure across the membrane wall [2,24]:

$$J = K\left(P_{f,m} - P_v\right) \quad (3)$$

where K is the mass transfer coefficient ($kg{\cdot}Pa^{-1}{\cdot}m^{-2}{\cdot}h^{-1}$), $P_{f,m}$ the feed vapor pressure at the membrane surface, and P_v the vacuum pressure on the permeate side. While K and P_v are almost constant in all cases, $P_{f,m}$ is exponentially related to temperature at the membrane surface ($T_{f,m}$) according to Antoine's equation [2].

Apparently, Fig. 3(a) and (b) show that applying ultrasonic energy using different values of power and frequency in the S-VMD improved the permeate flux relative to the case without ultrasonic energy, under similar feed temperatures. This finding is in line with previous research which reported improvement in permeate flux in S-VMD systems using other agitation techniques such as aeration or circulation [4,8]. It is important to note that, in submerged MD systems, the effect of temperature polarization is more significant due to the lack of turbulence relative to that in cross-flow MD systems. In other words, S-MD suffers from a larger difference between the feed temperature at the membrane surface and that at the bulk phase ($T_{f,b}$ - $T_{f,m}$) which is a result of the presence of a boundary layer and the heat loss due to evaporation at the membrane surface [25]. Thus, applying ultrasonic energy can reduce the effect of temperature polarization (i.e. lower boundary layer resistance) resulting in higher $T_{f,m}$ and therefore a higher permeate flux as described in Eq. (3).

In order to accurately measure the enhancement effect of ultrasound with different values of power and frequency, the permeate flux enhancement ratio Φ can be used:

$$\Phi = \frac{J_{US}}{J_{non-US}} \quad (4)$$

where J_{US} and $J_{non\text{-}US}$ are the measured permeate fluxes of the S-VMD with ultrasound and without ultrasound under the same operating conditions, respectively.

The values of Φ for two values of ultrasonic power and frequency under different $T_{f,b}$ is shown in Fig. 3(c). It is clear that, in general, applying higher power and lower frequency results in better values of Φ. This is in agreement with what is reported in the literature in ultrasonic-assisted MD systems under cross-flow configuration [16,18].

Moreover, it can be noted that the use of ultrasonic energy (under the same power and frequency) is more effective in terms of Φ with lower $T_{f,b}$. This occurred despite the fact that the effect of temperature polarization is expected to be higher at high values of $T_{f,b}$ [25] and so the ultrasonic energy is expected to perform better at higher $T_{f,b}$. This raises questions about dominating mechanisms associated with ultrasound enhancement in the S-VMD and the role the feed temperature plays. This is discussed in detail in the following section.

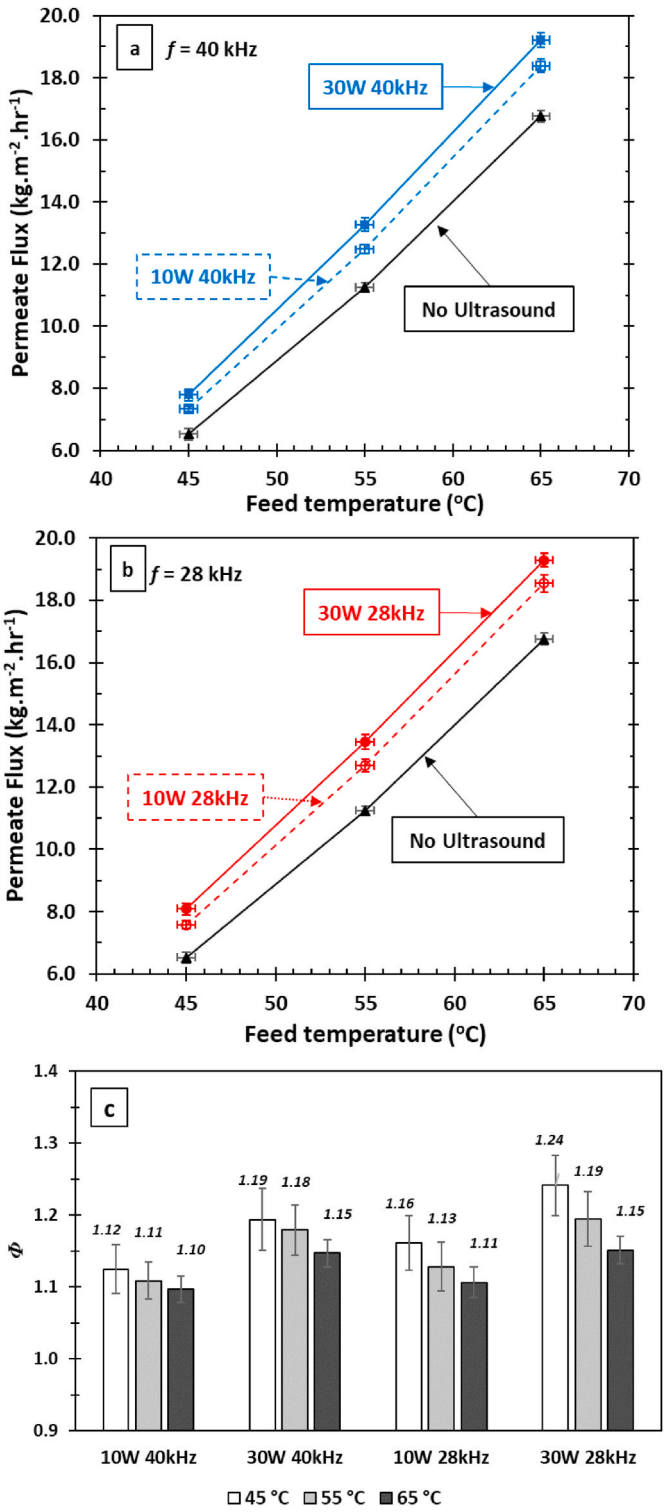

Fig. 3. Permeate flux J with and without ultrasound at (a) $f = 40$ kHz, and (b) $f = 28$ kHz, and (c) the flux enhancement ratio Φ ($P_v = -93.5 \pm 0.5$ kPa, Feed concentration = 35 g/l).

3.2. Identifying the ultrasonic enhancing mechanisms

The ultrasound-induced improvement in permeate flux can be explained through heat and mass transfer enhancing mechanisms associated with application of ultrasound in MD [14–16,18,21,26]. Commonly postulated in the literature and main contributor mechanisms to ultrasound-enhanced heat and mass transfer phenomena are *acoustic streaming* and *acoustic cavitation*, as well as other minor mechanisms including but not limited to *microstreaming*, *surface cavitation*, *turbulent boundary layer alteration*, and *enhanced diffusion* as a result of acoustic streaming and cavitation [11,12,27–35]. The real challenge is to identify the degree to which these mechanisms contribute to the enhancement. Investigating the effects of frequency at which ultrasound is applied is the key parameter to fundamentally understand the ultrasound-induced enhancement in permeate flux as acoustic streaming effects intensify with an *increase* in frequency and acoustic cavitation effects amplify with a *decrease* in frequency [28,31,32,36–38]. The ultrasonically induced kinematic momentum F resulting in acoustic streaming of a fluidic medium is defined as [31]:

$$F = \frac{\rho W_{US}}{c}\left(1 - e^{-2\alpha x}\right) \tag{5}$$

where ρ is the fluid density, c the speed of sound in the fluidic medium, W_{US} the ultrasonic power, α the acoustic attenuation coefficient of the fluidic medium and x the distance from the ultrasound emitting source. Considering an arbitrary point in the middle of the feed tank ($x = 0.1\ m$), the variation of kinematic momentum with frequency for both power levels and three feed water temperatures is depicted in Fig. 4(a). As it can be inferred from the figure, the ultrasonically induced kinematic momentum and consequently the acoustic streaming effect increases with an increase in frequency regardless of ultrasonic power and fluid temperature. If we consider acoustic streaming as the key player in enhancement of the permeate flux, the enhancement ratio (Φ) should increase with an increase in frequency. However, the results indicate an opposite trend as shown in Fig. 3(c) and values of Φ *decrease* with an increase in frequency. So, acoustic streaming can be disregarded as the key player in ultrasound-enhanced VMDs and its effects on permeate flux enhancement can be considered as insignificant.

Acoustic cavitation is the establishment and growth of gas/vapor-filled bubbles that move around and consequently implode violently to cause microstreaming. The movement and jet-like streams due to implosion of the cavitation bubbles result in enhanced heat and mass transfer [28,32,33,39–41]. The heat and mass transfer enhancement associated with cavitation-induced effects of ultrasound is proportional to the cavitation bubble critical radius; the larger the bubbles are the more disruption they cause upon movement and the more energy released upon collapse [42,43]. The critical radius R_{max} of a cavitation bubble, which is the bubble radius right before the implosion, is determined as [28]:

$$\omega^2 \rho R_{max}^2 = 3\mu\left(P_a - \frac{2\sigma}{R_{max}}\right) \tag{6}$$

where ω is the angular frequency ($\omega = 2\pi f$), μ the kinematic viscosity of the fluid, P_a the acoustic pressure, and σ the surface tension of the fluid. The values of critical bubble radius for all cases of ultrasonic power, ultrasonic frequency and feed water temperature are shown in Fig. 4(b). Comparing the trend in variations of Φ (Fig. 3(c)) and cavitation bubble critical radius (Fig. 4(b)) with regard to feed water temperature, ultrasonic power and ultrasonic frequency reveals an almost perfect hand-in hand similarity between the two: both increase as ultrasonic power increases and decrease when feed water temperature and ultrasonic frequency increase. The two are correlated with a coefficient of 95%. The inverse proportionality between permeate flux enhancement ratio and ultrasonic frequency suggests that acoustic cavitation is the dominant contributor to the observed enhancement.

3.3. The influence of feed temperature on the ultrasound-assisted enhancement

The decline in ultrasound-induced improvement in permeate flux with an increase in feed water temperature could be explained by the cavitation effect. The maximum pressure P_{max} and temperature T_{max} (i.

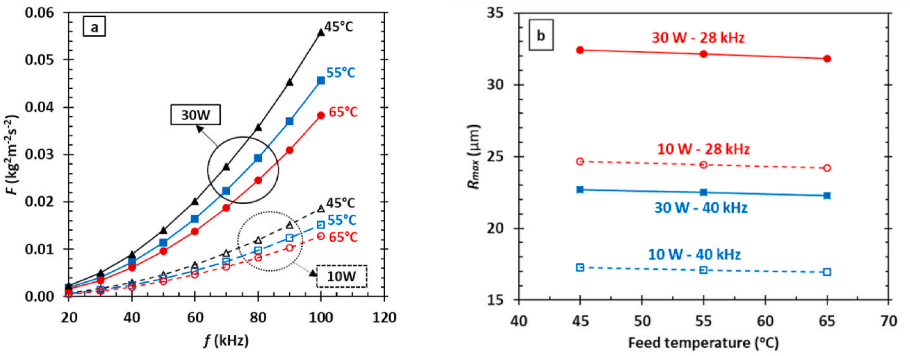

Fig. 4. The variation of kinematic momentum (a) and critical cavitation bubble radius (b) with ultrasonic power, frequency, and feed water temperature.

e., the implosion pressure and temperature) attained upon bursting of a cavitation bubble are obtained as [44,45]:

$$P_{max} = P_b \left(\frac{P_l(\gamma - 1)}{P_b} \right)^{\frac{\gamma}{\gamma - 1}} \tag{7}$$

$$T_{max} = T_l \left(\frac{P_l(\gamma - 1)}{P_b} \right) \tag{8}$$

where P_b is the pressure inside the bubble at its maximum size and is assumed to be equal to the vapor pressure of the liquid ($P_b = P_v@T_l$), P_l the instantaneous fluid pressure at the moment of collapse including hydraulic P_h and acoustic pressure ($P_l = P_h + P_a$), γ the specific heat ratio of the vapor/gas inside the bubble, and T_l the temperature of the fluid. With an increase in feed water temperature, the water vapor pressure increases resulting in lower implosion pressure and temperature (according to Eqs. (7) and (8)) and hence the decline in Φ [42,45].

3.4. The influence of ultrasonic frequency on the ultrasound-assisted enhancement

Although integration of ultrasound enhances the permeate flux, the frequency at which ultrasound is applied in order to achieve higher permeate flux is of major concern. As shown in Fig. 3(c), the values of Φ reduce when frequency increases from 28 kHz to 40 kHz regardless of ultrasonic power and feed water temperature. It is also noteworthy that a transducer of 120 kHz frequency was tried with a power of 30 W, but no significant improvements were observed suggesting that the ultrasonic power was not sufficient to initiate acoustic cavitation since the acoustic cavitation threshold increases with frequency [42,45,46].

This is because the effects of acoustic cavitation being the major contributor to the observed enhancement decreases as frequency increases [26,28,45]. It can be argued that as frequency increases, the rarefaction cycles become shorter, and the time period necessary for the rarefaction cycle becomes too short to allow bubbles to grow to a size sufficient to cause significant disturbances in the liquid [45]. The shortness of the time period of the compression half-cycle can also affect the cavitation if it becomes shorter than the time required for the bubble to collapse. Another possible reason can be the amount of ultrasonic energy delivered to the system. The acoustic intensity I is defined as:

$$I = 2\rho c \pi^2 \delta^2 f^2 \tag{9}$$

where δ is the acoustic displacement, and f is the ultrasonic frequency. For constant acoustic intensity in a medium, the acoustic displacement changes with frequency according to:

$$I_1 = I_2 \rightarrow \frac{\delta_2}{\delta_1} = \frac{f_1}{f_2} \tag{10}$$

Meaning that at constant ultrasonic intensity, acoustic displacement decreases linearly with an increase in frequency. The ultrasonic energy delivered by a transducer E_T is proportional to the acoustic displacement and is defined as [26,47]:

$$E_T = \frac{I}{c} \pi b^2 (2\delta) \tag{11}$$

where b is the transducer radius. So, under constant acoustic intensity, with an increase in frequency the delivered energy by the transducer decreases, and consequently the effectiveness of integration of ultrasound decreases resulting in lower Φ.

3.5. The performance of the ultrasonic-assisted S-VMD with feed concentration

The effect of the ultrasonic energy with different concentrations of NaCl solutions was also examined. In these experimental runs, the feed temperature was fixed at 55 °C, whereas the ultrasonic power and frequency were set at 30 W and 40 kHz, respectively. As shown in Fig. 5(a), the permeate flux declines with an increase in feed concentration with and without ultrasonic energy. This is expected as the presence of salt reduces the vapor partial pressure of the feed which negatively affects the driving force as described in Eq. (3). Moreover, the effect of concentration polarization (i.e. higher concentration at the membrane surface relative to that at the bulk phase of the feed) worsens as both the feed viscosity and the boundary layer thickness increase with higher feed concentration.

Fig. 5(a) also indicates that ultrasonic energy enhanced the permeate flux when compared to the case without ultrasonic energy at the same feed concentration. While the absolute values of J decreased with increasing the feed concentration as discussed above, the enhancement ratio Φ was better at higher concentration as shown in Fig. 5(b), which is consistent with what others reported in the literature [16,17]. This clearly suggests that ultrasonic energy can play a role in mitigating the effect of concentration polarization, which is mainly attributed to the cavitation effects that potentially enhance the mass transfer process at the membrane-liquid interface.

To clarify this, it is necessary to note that impurities and molecular discontinuity play a crucial role in acoustic cavitation. It is very difficult to induce cavitation in pure liquids and requires high levels of acoustic intensity to initiate acoustic cavitation. The presence of impurities and dissolved particles of particulate matter (level of hydrophobicity) provides nooks and crannies that could trap and host gas/vapor nuclei, thus lowering the cavitation threshold. Another advantage of impurities and dissolved particles is that they lower the surface tension of the liquid resulting in lower acoustic cavitation threshold [42].

3.6. Long-term operation

Membrane scaling represents a serious challenge particularly for S-VMD configuration [48]. Because of the lack of feed turbulence, inorganic salts can accumulate at a faster rate causing pore blocking and

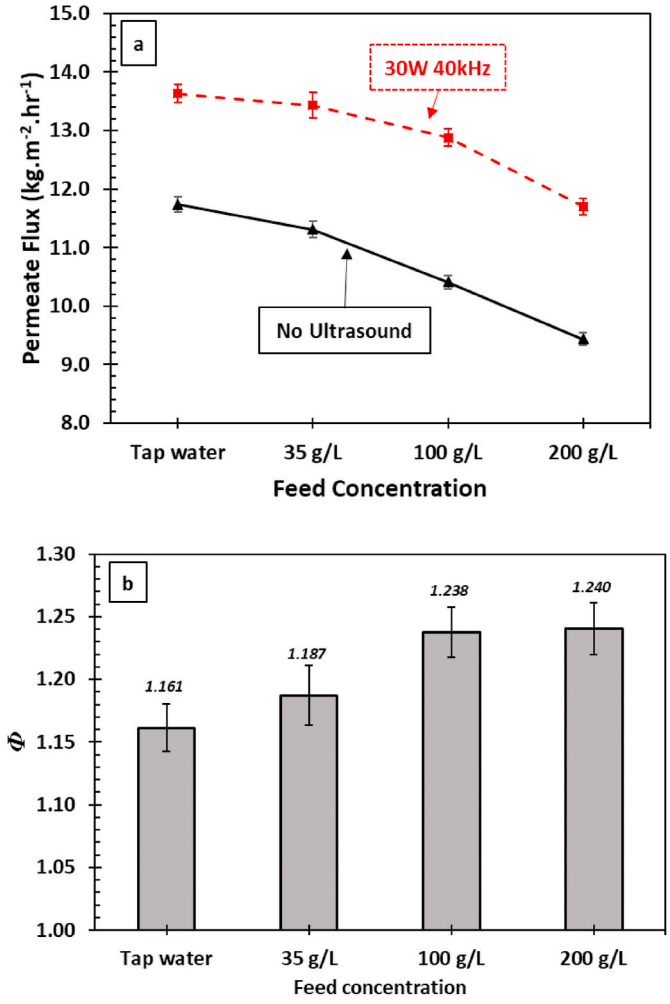

Fig. 5. (a) Permeate flux J and (b) the flux enhancement ratio Φ as a function of feed concentration with and without ultrasound. ($P_v = -93.5 \pm 0.5$ kPa, $T_{f,b} = 55$ °C, $W_{US} = 30$ W, and $f = 40$ kHz).

consequently reducing the permeate flux and its quality. While researchers reported that ultrasound significantly helped to mitigate membrane scaling in DCMD [18,19] and AGMD [15] systems under the cross-flow configuration, the effect of ultrasound to reduce membrane scaling in the submerged configuration is not clear yet. Moreover, it was reported that applying ultrasound in MD can cause structural damage and wetting of the membranes, especially if high power were used. Thus, it is important to investigate if applying ultrasonic energy in S-VMD would mitigate membrane scaling, and whether it causes structural damage of the membrane.

In this section, long-term tests (~15–16 h) were conducted with and without applying ultrasound using two new modules. Because of power restrictions, the ultrasonic transducer operates in an intermittent cycle (5 min ON - 5 min OFF). A synthetic NaCl solution with an initial concentration of 100 g/l was used as the feed water and its temperature was kept at 65 °C. As the feed volume decreases over time, 15 ml of the feed (at 100 g/l concentration) is added to the container every 10 min to keep the feed volume constant. When the feed concentration reached a point very close to the supersaturation limit (~350 g/l), the experiments were terminated.

Fig. 6 shows the variation of permeate flux and conductivity as a function of feed concentration factor (i.e. the ratio of the feed concentration at a certain time to the initial concentration) with and without ultrasound. As expected, the permeate flux in both cases gradually declined as the feed concentration increased with time. While the

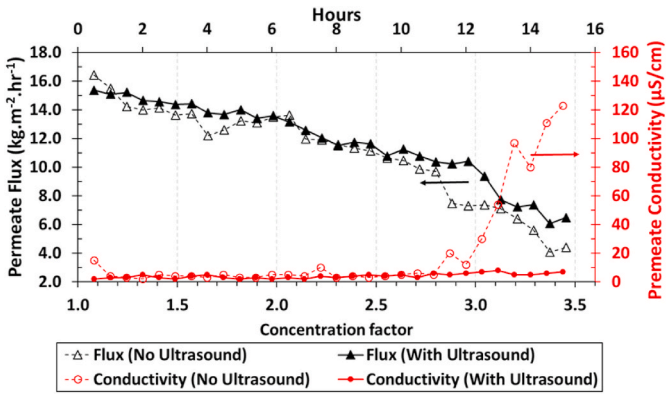

Fig. 6. The variation of permeate flux J and conductivity as a function of feed concentration factor with and without ultrasound. ($P_v = -93.5 \pm 0.5$ kPa, $T_{f,b} = 65$ °C, initial NaCl concentration = 100 g/l, $W_{US} = 30$ W, and $f = 40$ kHz).

permeate flux in both cases was very close when the concentration factor is less than 2.8, the case with ultrasound seems to perform better overall, but not significantly (up to 10% increase). This can be attributed to the intermittent nature of applying ultrasound in the long-term operation. Another reason is that the enhancement ratio after applying ultrasound is diminished with higher feed temperature, as discussed above.

Interestingly, as the concentration factor reached ~2.8, a rapid decline in the flux was observed in the test with no ultrasound. Starting from this point until the end of operation, the effect of ultrasound energy was more obvious as the permeate flux was remarkably higher compared to the case with no ultrasound. This can be explained as follows: as the concentration factor reaches a point close to supersaturation, the feed concentration on the membrane surface can be greater than the metastability limit of NaCl solution, considering the polarization effect. This can lead to accumulation and crystallization of salt on the membrane surface, which can consequently block the membrane pores and cause penetration of salt crystals into the pores. This phenomenon is especially problematic when there is no feed agitation [8] and can cause a rapid decrease in the flux as in the case with no ultrasound.

To evaluate this closely, SEM/EDS analysis was conducted at the end of each long-duration test. Fig. 7 shows SEM/EDS images of the membrane surface and cross section with and without applying ultrasound. The SEM images show larger salt crystals deposited on the membrane surface for the case without ultrasound. This could block the membrane pores and allow partial salt penetration to the permeate side. In the case with ultrasound, however, the deposition of salt on the membrane surface was relatively low. Moreover, the EDS analysis indicates a much lower deposition of sodium salts in the case with ultrasound. This indicates that applying ultrasound in an MD process can operate as a cleaning technique that mitigates membrane scaling as reported in the literature [14,20]. The agitation effects caused by the ultrasonic waves can continuously stimulate the feed-membrane interface, preventing the formation of salt crystals on the membrane surface.

With regard to the permeate quality, it can be seen in Fig. 6 that the permeate conductivity increased remarkably (up to 123 µS/cm) when the concentration factor reached ~3.1 in the test with no ultrasound, which is possibly caused by partial penetration of salt crystals. However, the conductivity was maintained well below the conductivity of drinkable water, which means that the membrane did not suffer from pore wetting. On the other hand, the salt rejection was very high in the ultrasonic test and the permeate quality was maintained below 10 µS/cm throughout the experiment. This indicates that ultrasound can mitigate salt crystallization on the membrane surface and prevent penetration of salt crystals into the pores. It also suggests that ultrasound did not cause pore wetting or structural damage of the membrane. In future work, it is important to investigate the effect of ultrasonic energy to mitigate

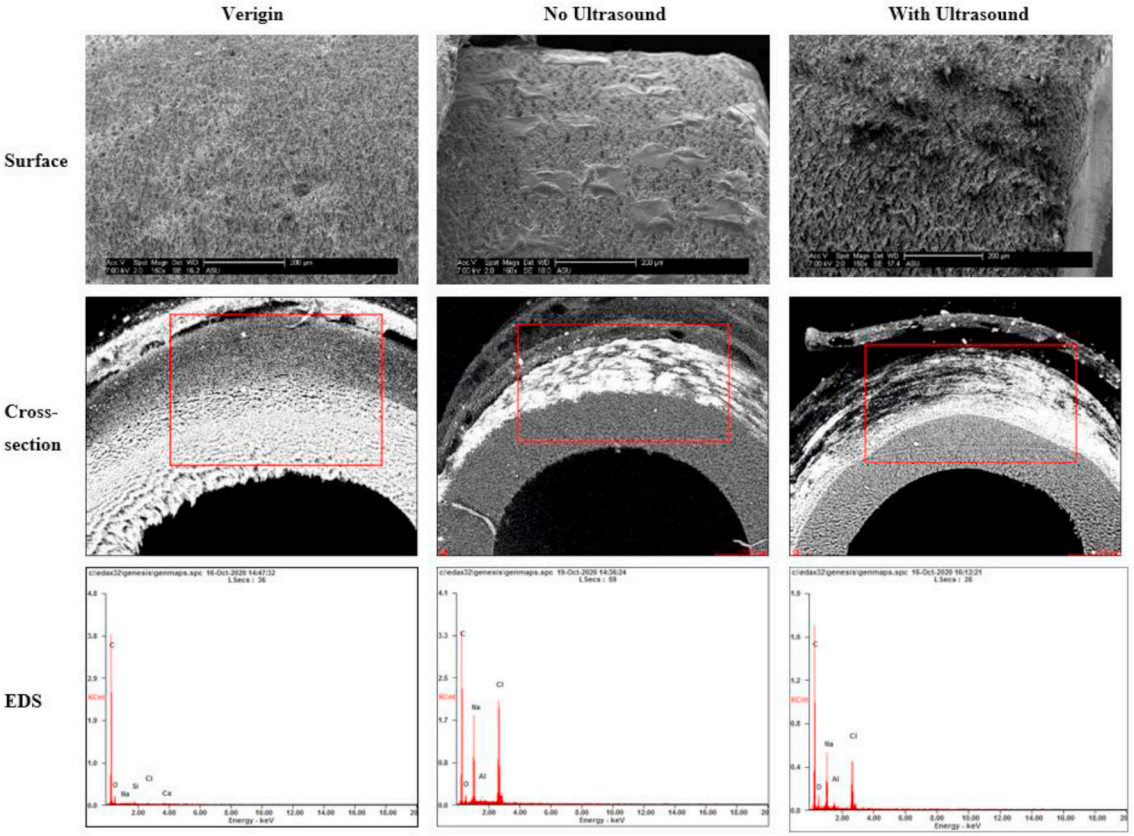

Fig. 7. SEM/EDS of membrane surface and cross section at the end of the long-duration test with and without ultrasound.

membrane scaling and fouling in a S-VMD system using even higher concentration feed water (e.g. inland brine or oil-produced water).

3.7. Ultrasonic enhancement in specific energy consumption (SEC)

While previous studies focused on how ultrasound can enhance permeate flux and mitigate fouling in MD processes, the effect of applying ultrasound on energy consumption was not apparently addressed. In other words, it is not yet clear whether the added power required to apply ultrasound can achieve better energy consumption per unit mass of distillate water produced.

In order to investigate this, the results obtained in section 3.1 are used to calculate the ultrasonic enhanced specific energy consumption (*UESEC*), which compares the specific energy consumption with applying ultrasound (SEC_{US}) to the case without ultrasound ($SEC_{NO\text{-}US}$):

$$UESEC = \frac{SEC_{NO-US} - SEC_{US}}{SEC_{NO-US}} \tag{12}$$

SEC calculates how much energy is required to produce a unit mass of freshwater (in kWh/kg). *SEC* is divided into specific thermal energy consumption (*STEC*) and specific electric energy consumption (*SEEC*) [49,50]:

$$SEC = STEC + SEEC \tag{13}$$

STEC can be defined as the amount of thermal energy ($\dot{Q}_{heat}$) required to produce a unit mass of distillate water ($\dot{m}_d$):

$$STEC = \frac{\dot{Q}_{heat}}{\dot{m}_d} = \frac{\dot{m}_{HTF} C_p \Delta T_{HTF}}{\dot{m}_d} \tag{14}$$

where $\dot{m}_{HTF}$ is the mass flow rate of the heat transfer fluid, C_p the specific heat, and ΔT_{HTF} the temperature drop of the heat transfer fluid in the heating coil.

Similarly, *SEEC* takes into account the total amount of electric energy required ($\dot{W}$):

$$SEEC = \frac{\sum \dot{W}}{\dot{m}_d} = \frac{\dot{W}_{vaccum} + \dot{W}_{US}}{\dot{m}_d} \tag{15}$$

where $\dot{W}$ is the combination of the power required for the ultrasonic transducer ($\dot{W}_{US}$) and that for the vacuum pump ($\dot{W}_{vaccum}$). For our lab-scale system, the rating power of the vacuum pump (168 W) is used for $\dot{W}_{vaccum}$ [49].

Fig. 8 illustrates the *UESEC* for different ultrasonic power and frequency at different feed temperatures according to Eq. (12). It is clear that applying ultrasound in the S-VMD system resulted in a better utilization of energy (i.e. less energy per unit mass of distillate water), which is similar to the observed enhancement in permeate flux (Fig. 3

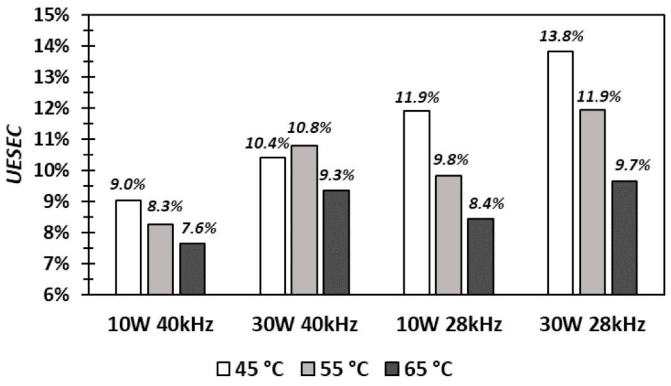

Fig. 8. Ultrasonic enhanced specific energy consumption (*UESEC*) ($P_v = -93.5 \pm 0.5$ kPa, Feed concentration = 35 g/l).

(c)). The values of *UESEC* were better with increasing the ultrasonic power from 10 W to 30 W, irrespective of the change in ultrasonic frequency or feed temperature. This indicates that the added power required to operate the ultrasonic transducers not only increases the amount of distillate water, but it is more effective in terms of energy consumption. These findings are in agreement with a recent study which found that feed agitation using circulating pumps in an S-VMD can enhance its energy efficiency [51].

4. Conclusions

The performance of an ultrasonic-assisted submerged vacuum membrane distillation (S-VMD) system was investigated experimentally. To do so, the effects of the ultrasonic power and frequency on the permeate flux were demonstrated under different feed temperatures and concentrations. Moreover, the effects of ultrasound energy in a relatively long-term operation using high concentration NaCl solution were also examined. From the investigations, the following conclusions were made:

- Applying low-power ultrasound in the S-VMD enabled it to improve the permeate flux when compared to the case without feed agitation (up to 24%).
- The enhancement ratio was more pronounced with an increase in the ultrasonic power and feed concentration as well as a decrease in the ultrasonic frequency and feed temperature.
- Based on the observed variation of the enhancement ratio with frequency, acoustic cavitation was identified as the dominant mechanism of the enhancement. The enhancement ratio and critical radius of the cavitation bubble was observed to be highly correlated ($R = 0.95$).
- The variation of the enhancement ratio with other parameters including feed temperature and salt concentration is in accordance with acoustic cavitation being the dominant mechanism behind the observed improvement.
- The intermittent application of ultrasound in a long-term operation resulted in a relatively higher permeate flux and better salt rejection when compared to the case with no ultrasound.
- Applying ultrasound was found to be more efficient in terms of total energy required to produce a unit mass of freshwater.
- Future work will be needed to study the effect of ultrasonic energy to mitigate membrane scaling and fouling in S-VMD systems using high concentration feed water with a large suspended solid content.

Credit author statement

Ahmad Bamasag: Conceptualization, Methodology, Investigation, Data Curation, Writing - Original Draft. **Hooman Daghooghi-Mobarakeh**: Conceptualization, Methodology, Investigation, Data Curation, Writing - Original Draft. **Talal Alqahtani:** Methodology, Investigation. **Patrick Phelan**: Resources, Writing - Review & Editing, Funding acquisition, Supervision.

Declaration of competing interest

The authors declare that they have no known competing financial interests or personal relationships that could have appeared to influence the work reported in this paper.

Acknowledgements

A. Bamasag gratefully acknowledges King Abdulaziz University (KAU) for supporting his study at Arizona State University (ASU), USA. This material is partially based upon work supported by the National Science Foundation under Grant Number CBET – 1703670. Any opinions, findings, and conclusions or recommendations expressed in this material are those of the authors and do not necessarily reflect the views of the National Science Foundation.

References

[1] E. Drioli, A. Ali, F. Macedonio, Membrane distillation: recent developments and perspectives, Desalination 356 (2015) 56–84, https://doi.org/10.1016/j.desal.2014.10.028.
[2] A. Alkhudhiri, N. Darwish, N. Hilal, Membrane distillation: a comprehensive review, Desalination 287 (2012) 2–18, https://doi.org/10.1016/j.desal.2011.08.027.
[3] P. Wang, T.S. Chung, Recent advances in membrane distillation processes: membrane development, configuration design and application exploring, J. Membr. Sci. 474 (2015) 39–56, https://doi.org/10.1016/j.memsci.2014.09.016.
[4] S. Meng, Y.C. Hsu, Y. Ye, V. Chen, Submerged membrane distillation for inland desalination applications, Desalination 361 (2015) 72–80, https://doi.org/10.1016/j.desal.2015.01.038.
[5] H. Julian, S. Meng, H. Li, Y. Ye, V. Chen, Effect of operation parameters on the mass transfer and fouling in submerged vacuum membrane distillation crystallization (VMDC) for inland brine water treatment, J. Membr. Sci. 520 (2016) 679–692, https://doi.org/10.1016/j.memsci.2016.08.032.
[6] Y. Choi, G. Naidu, S. Jeong, S. Vigneswaran, S. Lee, R. Wang, A.G. Fane, Experimental comparison of submerged membrane distillation configurations for concentrated brine treatment, Desalination 420 (2017) 54–62, https://doi.org/10.1016/j.desal.2017.06.024.
[7] W. Zhong, H. Li, Y. Ye, V. Chen, Evaluation of silica fouling for coal seam gas produced water in a submerged vacuum membrane distillation system, Desalination 393 (2016) 52–64, https://doi.org/10.1016/j.desal.2016.03.004.
[8] T. Zou, G. Kang, M. Zhou, M. Li, Y. Cao, Submerged vacuum membrane distillation crystallization (S-VMDC) with turbulent intensification for the concentration of NaCl solution, Separ. Purif. Technol. 211 (2019) 151–161, https://doi.org/10.1016/j.seppur.2018.09.072.
[9] L. Francis, N. Ghaffour, A.S. Al-Saadi, G.L. Amy, Submerged membrane distillation for seawater desalination, Desalin. Water Treat. 55 (2015) 2741–2746, https://doi.org/10.1080/19443994.2014.946716.
[10] A. Bamasag, T. Alqahtani, S. Sinha, N. Ghaffour, P. Phelan, Solar-heated submerged vacuum membrane distillation system with agitation techniques for desalination, Separ. Purif. Technol. 256 (2021) 117855, https://doi.org/10.1016/j.seppur.2020.117855.
[11] M. Legay, N. Gondrexon, S. Le Person, P. Boldo, A. Bontemps, Enhancement of heat transfer by ultrasound: review and recent advances, Int. J. Chem. Eng. 2011 (2011), https://doi.org/10.1155/2011/670108.
[12] H. Daghooghi-Mobarakeh, N. Campbell, W.K. Bertrand, P.G. Kumar, S. Tiwari, L. Wang, R. Wang, M. Miner, P.E. Phelan, Ultrasound-assisted regeneration of zeolite/water adsorption pair, Ultrason. Sonochem. 64 (2020) 105042, https://doi.org/10.1016/j.ultsonch.2020.105042.
[13] H. Daghooghi Mobarakeh, K. Bandara, L. Wang, R. Wang, P.E. Phelan, M. Miner, Low-Grade Heat Utilization through Ultrasound-Enhanced Desorption of Activated Alumina/Water for Thermal Energy Storage, 2020, https://doi.org/10.1115/POWER2020-16802.
[14] M. Qasim, N.N. Darwish, S. Mhiyo, N.A. Darwish, N. Hilal, The use of ultrasound to mitigate membrane fouling in desalination and water treatment, Desalination 443 (2018) 143–164, https://doi.org/10.1016/j.desal.2018.04.007.
[15] O. Naji, R.A. Al-juboori, L. Bowtell, A. Alpatova, N. Ghaffour, Direct contact ultrasound for fouling control and flux enhancement in air-gap membrane distillation, Ultrason. Sonochem. 61 (2020), https://doi.org/10.1016/j.ultsonch.2019.104816.
[16] C. Zhu, G.L. Liu, C.S. Cheung, C.W. Leung, Z.C. Zhu, Ultrasonic stimulation on enhancement of air gap membrane distillation, J. Membr. Sci. 161 (1999) 85–93, https://doi.org/10.1016/S0376-7388(99)00105-2.
[17] D. Hou, G. Dai, H. Fan, H. Huang, J. Wang, An ultrasonic assisted direct contact membrane distillation hybrid process for desalination, J. Membr. Sci. 476 (2015) 59–67, https://doi.org/10.1016/j.memsci.2014.11.028.
[18] D. Hou, Z. Wang, G. Li, H. Fan, J. Wang, H. Huang, Ultrasonic assisted direct contact membrane distillation hybrid process for membrane scaling mitigation, Desalination 375 (2015) 33–39, https://doi.org/10.1016/j.desal.2015.07.018.
[19] D. Hou, L. Zhang, C. zhao, H. Fan, J. Wang, H. Huang, Ultrasonic irradiation control of silica fouling during membrane distillation process, Desalination 386 (2016) 48–57, https://doi.org/10.1016/j.desal.2016.02.032.
[20] M.A.A. Hejazi, O.A. Bamaga, M.H. Al-Beirutty, L. Gzara, H. Abulkhair, Effect of intermittent operation on performance of a solar-powered membrane distillation system, Separ. Purif. Technol. 220 (2019) 300–308, https://doi.org/10.1016/j.seppur.2019.03.055.
[21] H. Cho, J. Choi, Y. Choi, S. Lee, Ultrasonic-assisted removal of inorganic scales in high-salinity wastewater treatment using membrane distillation, Desalin. Water Treat. 157 (2019) 383–392, https://doi.org/10.5004/dwt.2019.24043.
[22] S. Bell, A beginner's guide to uncertainty of measurement, Natl. Phys. Lab. (2004) 1–41, https://doi.org/10.1111/j.1468-3148.2007.00360.x.
[23] A. Bamasag, T. Alqahtani, S. Sinha, N. Ghaffour, P. Phelan, Experimental investigation of a solar-heated direct contact membrane distillation system using evacuated tube collectors, Desalination 487 (2020), https://doi.org/10.1016/j.desal.2020.114497.
[24] M. Khayet, Membranes and theoretical modeling of membrane distillation: a review, Adv. Colloid Interface Sci. 164 (2011) 56–88, https://doi.org/10.1016/j.cis.2010.09.005.

[25] A.S. Alsaadi, L. Francis, G.L. Amy, N. Ghaffour, Experimental and theoretical analyses of temperature polarization effect in vacuum membrane distillation, J. Membr. Sci. 471 (2014) 138–148, https://doi.org/10.1016/j.memsci.2014.08.005.
[26] C. Zhu, G. Liu, Modeling of ultrasonic enhancement on membrane distillation, J. Membr. Sci. 176 (2000) 31–41, https://doi.org/10.1016/S0376-7388(00)00426-9.
[27] J.L. Laborde, A. Hita, J.P. Caltagirone, A. Gerard, Fluid dynamics phenomena induced by power ultrasounds, Ultrasonics 38 (2000) 297–300, https://doi.org/10.1016/S0041-624X(99)00124-9.
[28] P. Gao, X. Zhou, B. Cheng, D. Zhang, G. Zhou, Study on heat and mass transfer of droplet cooling in ultrasound wave, Int. J. Heat Mass Tran. 107 (2017) 916–924, https://doi.org/10.1016/j.ijheatmasstransfer.2016.11.002.
[29] Y. Shen, K. Yasui, Z. Sun, B. Mei, M. You, T. Zhu, Study on the spatial distribution of the liquid temperature near a cavitation bubble wall, Ultrason. Sonochem 29 (2016) 394–400, https://doi.org/10.1016/j.ultsonch.2015.10.015.
[30] X. Ma, B. Huang, Y. Li, Q. Chang, S. Qiu, Z. Su, X. Fu, G. Wang, Numerical simulation of single bubble dynamics under acoustic travelling waves, Ultrason. Sonochem. 42 (2018) 619–630, https://doi.org/10.1016/j.ultsonch.2017.12.021.
[31] F.J. Trujillo, K. Knoerzer, A computational modeling approach of the jet-like acoustic streaming and heat generation induced by low frequency high power ultrasonic horn reactors, Ultrason. Sonochem. 18 (2011) 1263–1273, https://doi.org/10.1016/j.ultsonch.2011.04.004.
[32] B. Li, X. Han, Z. Wan, X. Wang, Y. Tang, Influence of ultrasound on heat transfer of copper tubes with different surface characteristics in sub-cooled boiling, Appl. Therm. Eng. 92 (2016) 93–103, https://doi.org/10.1016/j.applthermaleng.2015.09.069.
[33] H. Kiani, D.W. Sun, Z. Zhang, The effect of ultrasound irradiation on the convective heat transfer rate during immersion cooling of a stationary sphere, Ultrason. Sonochem. 19 (2012) 1238–1245, https://doi.org/10.1016/j.ultsonch.2012.04.009.
[34] D.W. Zhou, D.Y. Liu, X.G. Hu, C.F. Ma, Effect of acoustic cavitation on boiling heat transfer, Exp. Therm. Fluid Sci. 26 (2002) 931–938, https://doi.org/10.1016/S0894-1777(02)00201-7.
[35] K. Kerboua, O. Hamdaoui, Influence of reactions heats on variation of radius, temperature, pressure and chemical species amounts within a single acoustic cavitation bubble, Ultrason. Sonochem. 41 (2018) 449–457, https://doi.org/10.1016/j.ultsonch.2017.10.001.
[36] N. Riley, Acoustic streaming, Theor. Comput. Fluid Dynam. 10 (1998) 349–356, https://doi.org/10.1007/s001620050068.
[37] T. Thanh, Y. Asakura, S. Koda, K. Yasuda, Ultrasonics - Sonochemistry Dependence of cavitation , chemical e ff ect , and mechanical e ff ect thresholds on ultrasonic frequency vol. 39, 2017, pp. 301–306, https://doi.org/10.1016/j.ultsonch.2017.04.037.
[38] O. Bulliard-Sauret, J. Berindei, S. Ferrouillat, L. Vignal, A. Memponteil, C. Poncet, J.M. Leveque, N. Gondrexon, Heat transfer intensification by low or high frequency ultrasound: thermal and hydrodynamic phenomenological analysis, Exp. Therm. Fluid Sci. 104 (2019) 258–271, https://doi.org/10.1016/j.expthermflusci.2019.03.003.
[39] J. Cai, X. Huai, R. Yan, Y. Cheng, Numerical simulation on enhancement of natural convection heat transfer by acoustic cavitation in a square enclosure, Appl. Therm. Eng. 29 (2009), https://doi.org/10.1016/j.applthermaleng.2008.09.015, 1973–1982.
[40] N.P. Dhanalakshmi, R. Nagarajan, N. Sivagaminathan, B.V.S.S.S. Prasad, Chemical engineering and Processing : process intensification acoustic enhancement of heat transfer in furnace tubes, Chem. Eng. Process. Process Intensif. 59 (2012) 36–42, https://doi.org/10.1016/j.cep.2012.05.001.
[41] Y. Chen, S. Sun, Y. Lai, C. Ma, Influence of ultrasound to convectional heat transfer with fouling of cooling water, Appl. Therm. Eng. 100 (2016) 340–347, https://doi.org/10.1016/j.applthermaleng.2016.01.144.
[42] A.J. Walton, G.T. Reynolds, Sonoluminescence, Adv. Phys. 33 (1984) 595–660, https://doi.org/10.1080/00018738400101711.
[43] L.A. Crum, Acoustic cavitation series:part five:Rectified diffusion, Ultrasonics (1984) 215–223.
[44] S.K. Bhangu, M. Ashokkumar, Theory of sonochemistry, Top. Curr. Chem. 374 (2016) 1–28, https://doi.org/10.1007/s41061-016-0054-y.
[45] B.J.P. Lorimer, T.J. Mason, Sonochemistry:Part 1-The physical aspects *, Chem. Soc. Rev. 3 (1987) 239–274.
[46] S. Nomura, K. Murakami, Y. Aoyama, J. Ochi, Effects of change in frequency of ultrasonic vibrations on heat transfer, Nihon Kikai Gakkai Ronbunshu, B Hen/Trans. Japan Soc. Mech. Eng. Part B. 64 (1998) 1832–1838, https://doi.org/10.1299/kikaib.64.1832.
[47] S.A. Perusich, R.C. Alkire, Ultrasonically induced cavitation studies of electrochemical passivity and transport mechanisms: II . Experimental, J. Electrochem. Soc. 138 (1991) 708–713, https://doi.org/10.1149/1.2085662.
[48] H. Julian, Y. Ye, H. Li, V. Chen, Scaling mitigation in submerged vacuum membrane distillation and crystallization (VMDC) with periodic air-backwash, J. Membr. Sci. 547 (2018) 19–33, https://doi.org/10.1016/j.memsci.2017.10.035.
[49] C.K. Chiam, R. Sarbatly, Vacuum membrane distillation processes for aqueous solution treatment-A review, Chem. Eng. Process. - Process Intensif. 74 (2013) 27–54, https://doi.org/10.1016/j.cep.2013.10.002.
[50] R. Miladi, N. Frikha, A. Kheiri, S. Gabsi, Energetic performance analysis of seawater desalination with a solar membrane distillation, Energy Convers. Manag. 185 (2019) 143–154, https://doi.org/10.1016/j.enconman.2019.02.011.
[51] Y.S. Chang, B.S. Ooi, A.L. Ahmad, C.P. Leo, W.J. Lau, Numerical study on performance and efficiency of batch submerged vacuum membrane distillation for desalination, Chem. Eng. Res. Des. 163 (2020) 217–229, https://doi.org/10.1016/j.cherd.2020.08.031.